SCK • CEN
STUDIECENTRUM VOOR KERNENERGIE
CENTRE D'ÉTUDE DE L'ÉNERGIE NUCLÉAIRE

SCIENTIFIC REPORT
SCK•CEN-BLG-951

Power distribution in MOX fuel rods

Benchmark calculation

V. Kuzminov, E.Koonen

June, 2003

SCK•CEN
Boeretang 200
2400 Mol
Belgium

SCIENTIFIC REPORT OF THE BELGIAN NUCLEAR RESEARCH CENTRE
SCK•CEN-BLG-951

Power distribution in MOX fuel rods

Benchmark calculation

V. Kuzminov, E.Koonen

June, 2003
Status: Unclassified
ISSN 1379-2407

SCK•CEN
Boeretang 200
2400 Mol
Belgium

Distribution list

❒ P.Govaerts	1
❒ P.Gubel	1
❒ E. Koonen	3
❒ V. Kuzminov	5
❒ A.Beeckmans	1
❒ B.Ponsard	1
❒ S.Kaltcheva	1
❒ M.Verwerft	1
❒ L.Sannen	1
❒ V.Sobolev	1
❒ J.Dekeyser	1
❒ M.Weber	1
❒ L.Vermeeren	1
❒ A.Verwimp	1
❒ F.Gouat	1
❒ Th.Aoust	1
❒ B.Verboomen	1
❒ L.Borms	1
❒ Knowledge Centre	5
❒ BR2 Archive	5

		Date	Approval
Author	**V. Kuzminov**	17.06.2003	Kuzminov
Verified by:	**E. Koonen**	18.06.2003	E. Koonen
Approved by	**P. Gubel**	20.06.2003	P. Gubel

© SCK•CEN
Belgian Nuclear Research Centre
Boeretang 200
2400 Mol
Belgium
Phone +32 14 33 21 11
Fax +32 14 31 50 21

http://www.sckcen.be
Contact:
Knowledge Centre
library@sckcen.be

Power distribution in MOX fuel rods

Calculation of absolute values of linear power in MOX fuel rods irradiated in CALLISTO loop IPS1 in cycle 05/98a are presented in this report. The MCNP model of the high flux materials testing reactor BR2 was used for a simulation of the irradiation of MOX fuel rods. Calculations of the effective heating energy per fission in the irradiated MOX fuel rods were performed in order to determine the absolute values of the thermal power in MOX rods. The gamma-spectrometric measurements as well as the results from the thermal balance method are compared with the theoretical calculations. The calculated linear power distribution in MOX rods differs from the measured distribution on average not more than 5%.

Contents

1. Introduction

The experimental program in the high flux materials testing reactor BR2 includes the irradiation of various material samples as well as new types of fuel elements (rods, plates). An important characteristic for irradiation conditions of fuel elements is the power distribution. In the experiment involving the irradiation of 9 MOX fuel rods in the CALLISTO loop several methods were used to define the heating energy: thermal balance method, gross γ-spectrometry of measuring the distribution of fission products along the length of fuel rods, etc.

The thermal balance method [7] permits measurement on-line of the total heating energy in the CALLISTO loop. But the detailed distribution of heating energy in irradiated fuel rods is determined by using preliminary calculated power peaking factors. Various neutron transport codes may be applied for calculation of the radial and axial power peaking factors.
The γ-spectrometric measurement [1] of activity of fission products over the length of fuel rods provides information about the axial peaking power and the fission rate. The fission rate distribution in fuel rods can be measured with a high accuracy.

To compare the γ-spectrometric measurements and the thermal balance method of defining the heating energy in MOX rods, we have to know the effective heating energy per fission event peculiar to the irradiated MOX rods.

Calculations of the mean and the peak linear power distributions in MOX rods placed into the CALLISTO loop were performed using a very detailed MCNP model of BR2. The model includes a description of the real orientation of all inclined channels. The CALLISTO loop is located near the periphery of the BR2 core and contains thick stainless steel tubes, borate cooling water and a shroud tube of MOX fuel rods.

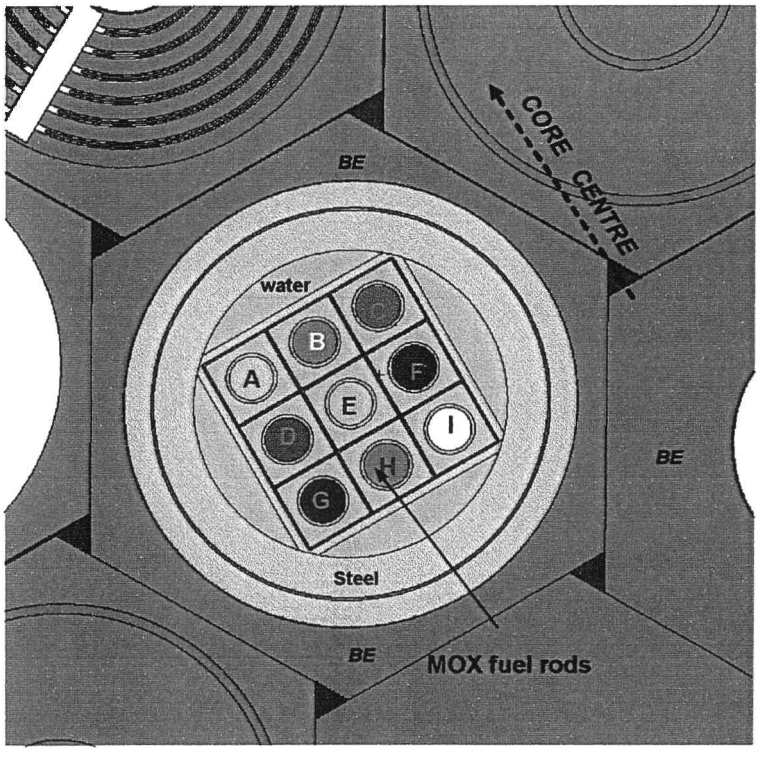

Fig. 1 CALLISTO loop containing MOX fuel rods inside a thick stainless steel tubes.

2. Technical specification of fresh MOX fuel rods

The starting nuclide composition of fresh fuel rods before the irradiation is shown in Tables 1,2. Nuclide composition is given in weight %. The cladding material in fuel rods is Zircaloy 4.

Table 1.Specification of MOX fuel in irradiated rods. Nuclide composition is given in weight %.

Rod name	F6547	F6548	F6549	F6673	F6674	F6677	F6678	F6679	F6680
Pellet lot	132/1	132/1	132/1	134/1	134/1	134/1	134/1	134/1	134/1
Rod position	A	B	C	G	I	F	E	H	D
Pellet diameter, cm	0.823	0.823	0.823	0.823	0.823	0.823	0.823	0.823	0.823
Length $(U,PU)O_2$, cm	100.2	100.2	100.2	100.08	99.78	99.75	100.41	100.42	100.66
Density g/cc	10.132	10.132	10.132	10.113	10.113	10.113	10.113	10.113	10.113
Pu/MOX	8.538	8.538	8.538	12.616	12.616	12.616	12.616	12.616	12.616
U/MOX	79.587	79.587	79.587	75.492	75.492	75.492	75.492	75.492	75.492
(Pu+U)/ MOX	88.125	88.125	88.125	88.108	88.108	88.108	88.108	88.108	88.108

Table 2. Specification of $(U,PU)O_2$ fuel in the fresh rods. Concentrations of U and Pu nuclides are given in weight % relative to U and to Pu, respectively.

Rod name	F6547	F6548	F6549	F6673	F6674	F6677	F6678	F6679	F6680
position	A	B	C	G	I	F	E	H	D
^{234}U	0.003	0.003	0.003	0.003	0.003	0.003	0.003	0.003	0.003
^{235}U	0.307	0.307	0.307	0.404	0.404	0.404	0.404	0.404	0.404
^{236}U	0.007	0.007	0.007	0.010	0.010	0.010	0.010	0.010	0.010
^{238}U	99.683	99.683	99.683	99.583	99.583	99.583	99.583	99.583	99.583
^{238}Pu	1.339	1.339	1.339	1.266	1.266	1.266	1.266	1.266	1.266
^{239}Pu	61.061	61.061	61.061	61.878	61.878	61.878	61.878	61.878	61.878
^{240}Pu	24.110	24.110	24.110	23.495	23.495	23.495	23.495	23.495	23.495
^{241}Pu	8.667	8.667	8.667	8.952	8.952	8.952	8.952	8.952	8.952
^{242}Pu	4.763	4.763	4.763	4.409	4.409	4.409	4.409	4.409	4.409

3. Irradiation history

MOX rods were initially irradiated in the BR3 reactor for 4000 hours and then in the BR2 reactor for 8 cycles. The irradiation history of MOX fuel rods is presented in Table 3. During the whole irradiation history in the BR2 reactor, the MOX rods resided in channel K49 of the CALLISTO loop.
In the present report we consider the irradiation of MOX fuel rods in the BR2 reactor operating cycle 05/98a. The nominal power of this cycle was P_{BR2}= 60.7 MW.

Table 3 Irradiation history of MOX fuel rods in the BR3 and BR2 reactors.

Reactor	Cycle	Reactor power, MW	Fuel rod name (position)		
			F6547 (A)	F6548 (B)	F6549 (C)
			Mean linear power in fuel rod, W/cm		
BR3	4d2	40.9	337	352	351
BR2	01/1997a	48.0	211	169	200
BR2	02/1997ab	59.1	188	179	164
BR2	03/1997a	56.2	210	178	214
BR2	01/1998a	50.8	201	176	205
BR2	02/1998a	56.2	210	187	212
BR2	03/1998a	56.7	191	172	196
BR2	04/1998a	58.3	181	162	185
BR2	05/1998a	60.8	191	170	193

Reactor	Cycle	Reactor power, MW	Fuel rod name (position)		
			F6673 (G)	F6674 (I)	F6677 (F)
			Mean linear power in fuel rod, W/cm		
BR3	4d2	40.9	225	225	256
BR2	01/1997a	48.0	182	167	173
	-				
BR2	03/1997a	56.2	185	186	189
BR2	01/1998a	50.8	176	175	183
BR2	02/1998a	56.2	191	189	197
BR2	03/1998a	56.7	169	171	180
BR2	04/1998a	58.3	166	166	173
BR2	05/1998a	60.8	176	174	180

Reactor	Cycle	Reactor power, MW	Fuel rod name (position)		
			F6678 (E)	F6679 (H)	F6680 (D)
			Mean linear power in fuel rod, W/cm		
BR3	4d2	40.9	228	228	259
BR2	01/1997a	48.0	132	136	187
	-				
BR2	03/1997a	56.2	140	145	186
BR2	01/1998a	50.8	142	141	182
BR2	02/1998a	56.2	156	154	198
BR2	03/1998a	56.7	142	138	177
BR2	04/1998a	58.3	136	134	171
BR2	05/1998a	60.8	143	142	181

4. Fuel composition of MOX rods in BOC 05/98A

The variation of nuclide composition in MOX fuel rods during the irradiation history was calculated by Ch. De Raedt and used in previous calculations of power distribution in MOX rods [2,3]. The following nuclide compositions in MOX fuel rods were used for calculating the power distribution at the beginning of fuel cycle 05/98a. Table 4 contains the atomic concentrations for each MOX fuel rod with an indication of the rod position in the CALLISTO loop.

The uniform axial distribution of Pu nuclides over the length of MOX fuel element was used in the computational model.

Table 4 Fuel composition for MOX rods in the BOC 05/98a. Atomic concentrations are given in units $cm^{-1}barn^{-1}$.

nuclide	Rod position				
	A	B	C	D	E
^{235}U	4.766×10^{-5}	4.825×10^{-5}	4.766×10^{-5}	6.760×10^{-5}	6.883×10^{-5}
^{236}U	3.464×10^{-6}	3.368×10^{-6}	3.449×10^{-6}	2.885×10^{-6}	2.755×10^{-6}
^{238}U	2.010×10^{-2}	2.010×10^{-2}	2.010×10^{-2}	1.988×10^{-2}	1.989×10^{-2}
^{239}Pu	8.213×10^{-4}	8.428×10^{-4}	8.214×10^{-4}	1.557×10^{-3}	1.639×10^{-3}
^{240}Pu	5.538×10^{-4}	5.512×10^{-4}	5.546×10^{-4}	7.826×10^{-4}	7.779×10^{-4}
^{241}Pu	1.466×10^{-4}	1.469×10^{-4}	1.455×10^{-4}	1.954×10^{-4}	1.911×10^{-4}
^{242}Pu	1.187×10^{-4}	1.174×10^{-4}	1.188×10^{-4}	1.483×10^{-4}	1.447×10^{-4}
^{241}Am	1.008×10^{-4}	1.021×10^{-4}	1.010×10^{-4}	1.447×10^{-4}	1.432×10^{-4}
^{243}Am	3.376×10^{-6}	3.255×10^{-6}	3.227×10^{-6}	2.808×10^{-6}	2.564×10^{-6}
^{244}Cm	1.359×10^{-7}	1.215×10^{-7}	1.258×10^{-7}	7.214×10^{-8}	5.733×10^{-8}
^{10}B	1.120×10^{-5}	1.070×10^{-5}	1.120×10^{-5}	1.220×10^{-5}	8.660×10^{-6}

nuclide	Rod position			
	F	G	H	I
^{235}U	6.763×10^{-5}	6.817×10^{-5}	6.881×10^{-5}	6.825×10^{-5}
^{236}U	2.868×10^{-6}	2.842×10^{-6}	2.732×10^{-6}	2.820×10^{-6}
^{238}U	1.988×10^{-2}	1.988×10^{-2}	1.989×10^{-2}	1.989×10^{-2}
^{239}Pu	1.557×10^{-3}	1.604×10^{-3}	1.635×10^{-3}	1.606×10^{-3}
^{240}Pu	7.832×10^{-4}	7.845×10^{-4}	7.800×10^{-4}	7.845×10^{-4}
^{241}Pu	1.947×10^{-4}	1.903×10^{-4}	1.898×10^{-4}	1.897×10^{-4}
^{242}Pu	1.483×10^{-4}	1.464×10^{-4}	1.451×10^{-4}	1.464×10^{-4}
^{241}Am	1.448×10^{-4}	1.421×10^{-4}	1.434×10^{-4}	1.423×10^{-4}
^{243}Am	2.703×10^{-6}	2.504×10^{-6}	2.324×10^{-6}	2.387×10^{-6}
^{244}Cm	6.708×10^{-8}	5.867×10^{-8}	4.830×10^{-8}	5.373×10^{-8}
^{10}B	1.210×10^{-5}	1.170×10^{-5}	1.020×10^{-5}	1.156×10^{-5}

5. Calculation of the thermal power in MOX fuel rods

The MCNP code [5] is used for calculating the distribution of the neutron flux density in MOX fuel rods. The length L (and the volume V_B) for various fuel rods differ slightly from each other. The number of fission reactions in the fuel rod, n_f^B [fissions per fission neutron in BR2], is defined as

$$n_f^B = \sum_i \int_E \int_{V_B} n_i \sigma_f^i(E) \Phi(r,E) dE dr, \qquad (1)$$

where n_i [1/cm^3] is the atomic concentration of nuclide i in the MOX fuel, $\sigma_f^i(E)$ [cm^2] is the microscopic cross-section for the fission reaction of the nuclide i, $\Phi(r,E)$ [cm^{-2}eV^{-1}] is the neutron flux density calculated by MCNP and normalised per one fission neutron in BR2. The value of n_f^B is normalised per one fission neutron released in BR2. We need to have the number of fission reactions in the fuel rod during the whole cycle (normalised per produced energy in BR2) and also the effective duration of the cycle.

To define the normalization factor N_n let us consider the balance equation for energy E_{BR2} produced in BR2

$$E_{BR2} = Q_{eff}^{BR2} \left(\sum_i \int_E \int_{V_{BR2}} n_i \sigma_f^i(E) \Phi(r,E) dE dr \right) N_n, \qquad (2)$$

where Q_{eff}^{BR2} [eV/fission] (1 eV=1.602×10^{-19} Joules), is the effective energy released per fission reaction in BR2. The value in brackets in Eq.(2) is the total number of fission reactions in the BR2 per one fission neutron. From Eq.(2) we obtain the normalization factor N_n

$$N_n = \frac{E_{BR2}}{Q_{eff}^{BR2} \left(\sum_i \int_E \int_{V_{BR2}} n_i \sigma_f^i(E) \Phi(r,E) dE dr \right)} \qquad (3)$$

The 'effective' duration of cycle, T, is equal to the total energy produced in BR2 [MWdays] divided by the nominal power P_{BR2} [MW] of BR2

$$T = \frac{E_{BR2}}{P_{BR2}}$$

Let us rewrite the equation (3)

$$N_n = \frac{P_{BR2} T}{Q_{eff}^{BR2} \left(\sum_i \int_E \int_{V_{BR2}} n_i \sigma_f^i(E) \Phi(r,E) dE dr \right)} \qquad (4)$$

The total number of fission neutrons in the critical state of BR2 is equal to

$$S_n = \frac{1}{k_{eff}} \sum_i \int_E \int_{V_{BR2}} \nu_i n_i \sigma_f^i(E) \Phi(r,E) \, dE dr \, N_n, \qquad (5)$$

where ν_i is the number of neutrons released in the fission of nuclide i, and k_{eff} is the effective multiplication factor calculated by the code MCNP (for computer model of BR2).

Substituting the value of normalization factor N_n into Eq.(5) we have the equation for the total number of fission neutrons in BR2

$$S_n = \frac{\nu_{BR2}\,\mathrm{P}_{BR2}\,\mathrm{T}}{k_{eff} Q_{eff}^{BR2}},$$

where
$$\nu_{BR2} = \frac{\sum_i \int_E \int_{V_{BR2}} \nu_i n_i \sigma_f^i(E)\Phi(r,E)\,dE\,dr}{\sum_i \int_E \int_{V_{BR2}} n_i \sigma_f^i(E)\Phi(r,E)\,dE\,dr}, \qquad (6)$$

here ν_{BR2} is the mean number of neutrons released in BR2 per fission reaction (for BR2 ν_{BR2}=2.43 n/fiss).

The intensity of fission neutrons [neutrons/sec] in BR2 is equal to

$$\mathrm{I}_n^{BR2} = \frac{S_n}{\mathrm{T}} = \frac{\nu_{BR2}\,\mathrm{P}_{BR2}}{k_{eff} Q_{eff}^{BR2}}, \qquad (7)$$

where Q_{eff}^{BR2}=196 MeV =196×1.602×10^{-13} J (for details of calculations see below).

Finally, the power in the fuel rod normalized per nominal BR2 power is obtained by using Eq.(1) for the number of fission reactions and the intensity, I_n^{BR2}, of fission neutrons in BR2

$$\mathrm{P}_B = Q_{eff}^B n_f^B \mathrm{I}_n^{BR2} = Q_{eff}^B \frac{\nu_{BR2}\mathrm{P}_{BR2}}{k_{eff} Q_{eff}^{BR2}} \left(\sum_i \int_E \int_{V_B} n_i \sigma_f^i(E)\Phi(r,E)\,dE\,dr \right), \qquad (8)$$

where Q_{eff}^B is the effective heating energy per fission event in the fuel rods.

The linear power in the fuel rods [W/cm] is calculated as the ratio of the power P_B to the length L of the fuel rods.

To obtain the thermal power in fuel rods we have additionally to know the effective heating energy, Q_{eff}^B, for irradiated MOX fuel rods and Q_{eff}^{BR2} value for the BR2 reactor. Below detailed calculations of the effective heating energy in irradiated MOX rods are presented.

6. Total effective energy released in fission

A detailed discussion of the effective energy Q_{eff} released in the fission reaction for fissionable nuclides of U, Pu was considered in the paper of M.James[4]. The recommended values of the useful energy released in fissionable materials include the kinetic energy of fission fragments, E_k; and total kinetic energies of all emitted neutrons, E_n; photons (prompt-E_γ^f, and delayed- E_γ^d) and beta particles, E_β. In Table 5 the corresponding components of the effective fission energy for ^{235}U and ^{239}Pu are presented. The total effective energy is

$$Q_{eff} = E_k + E_\beta + E_\gamma^f + E_\gamma^d + E_n - \Delta E_{\beta\gamma} - E_\nu, \qquad (9)$$

where $\Delta E_{\beta\gamma}$ is the energy released after the mean life of the fuel and E_ν is the energy of the antineutrino. For the life of fuel greater than 3 years, $\Delta E_{\beta\gamma}$ is about 0.17 MeV/fiss for ^{235}U [4]. The effective fission energy for ^{239}Pu is higher than for ^{235}U by 3%.

Table 5. Contributors to the effective energy Q_{eff} (MeV/fission) released in fission of ^{235}U and ^{239}Pu by thermal neutrons and in ^{238}U by fission spectrum neutrons [4].

Contribution	^{235}U (thermal neutrons)	^{238}U (fission neutrons)	^{239}Pu (thermal neutrons)
Kinetic energy of fission fragments, E_k	166.2 ± 1.3	166.9± 1.3	172.8 ± 1.9
Energy of prompt photons emitted after fission, E_γ^f	8.0 ± 0.8	7.5 ± 1.3	7.7 ± 1.4
Energy of delayed photons emitted with β-particles, E_γ^d	7.2 ± 1.1	8.4 ± 1.6	6.1 ± 1.3
Kinetic energy of β-particles, E_β	7.0 ± 0.3	8.9 ± 0.6	6.1 ± 0.6
Kinetic energy of fission neutrons, E_n	4.8 ± 0.1	5.5 ± 0.1	5.9 ± 0.1
Effective energy for fission reaction, Q_{eff}, *Eq.* (9)	192.9 ± 0.5	193.9 ± 0.8	198.5 ± 0.8

The emitted fission neutrons can undergo a capture reaction during their slowing down in the fuel or in various structural materials. In addition to fission energy useful for heating, the energy of photons produced in the neutron capture reaction should be taken into account. In Table 6 the average energy released with photons in the case of neutron capture are presented for various materials. The energy released after the neutron capture reaction depends on the probability of the capture reaction, $p_c = \sigma_c/\sigma_f$ (σ_c and σ_f are neutron capture and fission cross-sections). This energy is equal to $p_c Q^c$ and is dissipated in the surrounding materials (the values of Q^c for fuel are presented in Table 6).

Table 6. Effective Q^c-values for neutron capture for various materials.

Material	Effective Q^c -value (MeV/capture)	Material	Effective Q^c -value (MeV/capture)
^{235}U	6.54	H	2.22
^{238}U	5.69	O	3.38
^{239}Pu	6.53	Al	10.74
^{240}Pu	5.24	Fe	7.8
^{241}Pu	6.31	Steel	8.37
^{242}Pu	5.24	Zr	8.07

The effective energy for fission reaction includes the kinetic energies of all emitted particles that are dissipated in the fuel or in surrounding structural materials. The problem is to determine the effective heating energy Q_{eff}^{B} normalised per fission in a single fuel rod irradiated in the Callisto loop in the BR2 reactor.

The Callisto loop is located near the periphery of the BR2 reactor core and contains two thick stainless steel tubes, inside the inner tube are placed nine MOX fuel rods (see Fig.1). The value of the effective heating energy per fission event in MOX fuel rods differs from the total fission energy released in fuel elements in the BR2 reactor core. The first reason for this is that the MOX fuel contains Pu nuclides, while the fuel elements in the core of BR2 contain highly enriched U. The probabilities of neutron capture and photon generation in MOX fuel rods and in the BR2 core are different. The second reason is that MOX fuel rods have a small diameter and photons produced escape partly from fuel rods. Due to the leakage of photons from the fuel rods only a fraction of the total energy of photons produced in fission and capture reactions is absorbed in the MOX fuel rods. The remaining part of their energy is mainly absorbed in the thick pressure tubes (the wall thickness of the stainless steel tubes is equal to 1.0 cm). It should be noted that the effective mean Q_{eff}-value published in the literature for fission of nuclides of U and Pu includes the whole energy of all secondary particles.

The Monte Carlo code MCNP gives the possibility to calculate the fission energy deposition in various zones containing fissionable materials. The effective fission heating Q_F -values used in MCNP code for different fissionable materials are presented in Table 7. As can be seen, Q_F -value contains the energy of charged fission fragments E_k, the energy of β-particles, E_β, and the energy of delayed photons produced in β-decay reactions of fission fragments E_γ^d. To check this we will consider separate components of the Q_F -value using the results in paper [4].

The kinetic energy of fission fragments and of β-particles produced in the secondary decay reactions is deposited locally. It is assumed also that the whole energy of delayed photons from the decay of fission fragments is absorbed locally in the fuel. The recommended values for each of these components were taken from [4] and are compared in Table 7 with the values used in the MCNP code [5]. Energy of prompt photons produced in fission and capture reactions is not included into Q_F –value. The heating energy from prompt photons is simulated in the MCNP code independently in the coupled neutron-photons transport calculation.

Table 7. Fission heating Q_F -values used in the MCNP code.

	M.James [4]				MCNP [5]
	Fission Fragments				
Nuclide	E_k, Mev/fiss	E_β, MeV/fiss	E_γ^d, MeV/fiss	$Q_F = E_k + E_\beta + E_\gamma^d$, MeV/fiss	Q_F, MeV/fiss
^{235}U	166.2±1.3	7.0±0.3	7.2±1.1	180.4	180.88
^{238}U	166.9±1.3	8.9±0.6	8.4±1.6	184.2	181.31
^{239}Pu	172.8±1.9	6.1±0.6	6.1±1.3	185.0	189.44
^{241}Pu	172.2±2.2	7.4±0.6	7.4±1.5	187.0	188.99

As can be seen from Table 7, Q_F -values for ^{235}U used in MCNP and in [4] are close to each other. The difference in the fission heating Q_F-values for plutonium and uranium in the MCNP code is about 4.7 %, while according to [4] this difference is equal to 2.5%.

The heating energy, Q_F , includes the total energy of delayed photons. But in small fuel rods only a fraction of their energy is deposited inside the rod. The remaining fraction of the photon's energy is dissipated outside the fuel rod.

In order to determine the mean effective heating energy in MOX rods per fission in MOX we will consider the various components of the heating energy in the MOX fuel rods and in various structural elements.

7. Calculation of the effective fission energy for MOX rods

The following contributors to the heating energy are considered for determining the effective heating energy, Q_{eff}^{B}, for MOX fuel rods:

- The kinetic energy of fission fragments, E_k. The track length of fission fragments is small and all energy of fission fragments is deposited locally (absorbed) in fuel rods;
- The loss of the kinetic energy of fission neutrons, Q_n, in elastic and inelastic collisions in fuel rods during their slowing down.
- The energy of β-particles, E_β, produced in decay reactions of fission fragments (we assume that all their energy is deposited locally)
- The heating energy of prompt gammas, Q_γ^B, produced in fission and capture reactions
- The heating energy of delayed gammas coming from fission products in BR2 fuel elements, $Q_{\gamma,BR2}^{d}$, and generated in MOX rods, $Q_{\gamma,B}^{d}$.

Charged fission fragments and beta-particles deposit their energy locally, while the prompt and delayed photons may escape from the fuel rod and interact with structural elements surrounding the fuel rod. To estimate the effect of the photon leakage from the MOX fuel rods, calculations of their heating energy were performed using the MCNP and the SCALE codes.

7.1 Heating energy of photons

The γ-heating energy in MOX fuel rods is determined as

$$E_\gamma = \int_E \int_{V_B} \varphi^\gamma(r,E) H_\gamma(E) dE d^3r, \qquad (10)$$

where $\varphi^\gamma(r,E)$ is the gamma flux density and $H_\gamma(E)$ is a heat response, V_B is the volume of the MOX rod. Gamma flux density is determined using a Monte Carlo method of solving the integral equation for density collision function $\psi^\gamma(r,E)=\Sigma^\gamma_{tot}(r,E)\,\varphi^\gamma(r,E)$

$$\psi^\gamma(r,E,\Omega) = q_1^\gamma(r,E,\Omega) + \iiint \psi^\gamma(r',E',\Omega') K_\gamma(r',E',\Omega' \to r,E,\Omega) d^3r' dE' d\Omega', \quad (11)$$

where Σ^γ_{tot} is the total macroscopic cross-section; the density of first collisions, q_1^γ, can be written separately for the prompt and delayed photons

$$q_1^\gamma(r,E,\Omega) = \int_V q_\gamma(r,E,\Omega) T_\gamma(r' \to r;E,\Omega) d^3r' = q_1^{p,\gamma}(r,E,\Omega) + q_1^{d,\gamma}(r,E,\Omega), \qquad (12)$$

where $K_\gamma(r',E',\Omega' \to r,E,\Omega)$ and $T_\gamma(r' \to r;E,\Omega)$ are the transport kernels describing the photon interactions and transport in the medium. The forms of these kernels are not discussed here.
The gamma source $q_\gamma(r,E,\Omega)$ in Eq.(12) can be represented as a sum of separate components for prompt and delayed gammas

$$q_\gamma(r,E,\Omega) = q_\gamma^p(r,E,\Omega) + q_\gamma^d(r,E,\Omega) \qquad (13)$$

The prompt γ is produced in the fission and capture reactions

$$q_\gamma^p(r,E,\Omega) = q_\gamma^{p,f}(r,E,\Omega) + q_\gamma^{p,c}(r,E,\Omega) \qquad (14)$$

In more details the sources for prompt γ have the form

$$q_\gamma^{p,f}(r,E,\Omega)=\chi_f^{p,\gamma}(E)\int_E \Sigma_f(r,E)\Phi_n(r,E)dE \qquad (15a)$$

$$q_\gamma^{p,c}(r,E,\Omega)=\chi_c^{p,\gamma}(E)\int_E \Sigma_c(r,E)\Phi_n(r,E)dE, \qquad (15b)$$

where the integral represents the fission density and the functions $\chi_f^{p,\gamma}$ and $\chi_c^{p,\gamma}$ are the spectra of prompt photons in fission and capture reactions, $\Phi_n(r,E)$ is the neutron flux density.
The source of delayed photons can be defined separately in the BR2 fuel elements and in MOX rods because there is no spatial migration of fission products in the core

$$q_{\gamma,B}^{d}(r,E,\Omega)=\chi_f^{d,\gamma}(E)\int_E \Sigma_f(r,E)\Phi_n(r,E)dE, \qquad r\in V_B \qquad (16)$$

$$q_{\gamma,BR2}^{d}(r,E,\Omega)=\chi_f^{d,\gamma}(E)\int_E \Sigma_f(r,E)\Phi_n(r,E)dE, \qquad r\in V_{BR2} \qquad (17)$$

The density of first collisions for prompt photons contains the components of γ-source produced in fission and neutron capture reactions

$$q_1^{p,\gamma}(r,E,\Omega)=\int_V q_\gamma^{p,f}(r,E,\Omega)T_\gamma(r'\to r;E,\Omega)d^3r'+\int_V q_\gamma^{p,c}(r,E,\Omega)T_\gamma(r'\to r;E,\Omega)d^3r' \qquad (18)$$

The density of first collisions for delayed photons has the form

$$q_1^{d,\gamma}(r,E,\Omega)=\int_V q^{d,\gamma}(r,E,\Omega)T_\gamma(r'\to r;E,\Omega)d^3r \qquad (19)$$

After considering separately the fission product in MOX and in BR2 fuel elements we can rewrite the density $q_1^{d,\gamma}$ ($V=V_{BR2}\cup V_B$, where V_{BR2} is the region of BR2 fuel elements, V_B is the region of MOX rods)

$$q_1^{d,\gamma}(r,E,\Omega)=\int_{V_{BR2}} q_{\gamma,BR2}^{d}(r,E,\Omega)T_\gamma(r'\to r;E,\Omega)d^3r'+\int_{V_B} q_{\gamma,B}^{d}(r,E,\Omega)T_\gamma(r'\to r;E,\Omega)d^3r' \qquad (20)$$

We can represent the collision density ψ^γ as a sum of components for prompt and delayed γ

$$\psi^\gamma(r,E,\Omega)=\psi^{p,\gamma}(r,E,\Omega)+\psi_{BR2}^{d,\gamma}(r,E,\Omega)+\psi_B^{d,\gamma}(r,E,\Omega) \qquad (21)$$

Substituting this representation of collision density into Eq.(11) we have

$$\psi^{p,\gamma}(r,E,\Omega)+\psi_{BR2}^{d,\gamma}(r,E,\Omega)+\psi_B^{d,\gamma}(r,E,\Omega)=q_1^{p,\gamma}(r,E,\Omega)+q_{1,BR2}^{d,\gamma}(r,E,\Omega)+q_{1,B}^{d,\gamma}(r,E,\Omega)+$$
$$\iiint\left(\psi^{p,\gamma}(r',E',\Omega')+\psi_{BR2}^{d,\gamma}(r',E',\Omega')+\psi_B^{d,\gamma}(r',E',\Omega')\right)K_\gamma(r',E',\Omega'\to r,E,\Omega)d^3r'dE'd\Omega', \qquad (22)$$

The solution of the Eq.(22) can be obtained from the separate equations for each constituent components of ψ^γ : for collision densities of prompt photons in the whole region and for the delayed photons produced in BR2 fuel elements and in MOX fuel rods. Then for each component we have to solve separate equations

$$\psi^{p,\gamma}(r,E,\Omega)=q_1^{p,\gamma}(r,E,\Omega)+\iiint\psi^{p,\gamma}(r',E',\Omega')K_\gamma(r',E',\Omega'\to r,E,\Omega)d^3r'dE'd\Omega', \qquad (23)$$

$$\psi_{BR2}^{d,\gamma}(r,E,\Omega)=q_{1,BR2}^{d,\gamma}(r,E,\Omega)+\iiint\psi_{BR2}^{d,\gamma}(r',E',\Omega')K_\gamma(r',E',\Omega'\to r,E,\Omega)d^3r'dE'd\Omega', \qquad (24)$$

$$\psi_B^{d,\gamma}(r,E,\Omega) = q_{1,B}^{d,\gamma}(r,E,\Omega) + \iiint \psi_B^{d,\gamma}(r',E',\Omega') K_\gamma(r',E',\Omega' \to r,E,\Omega) d^3r' dE' d\Omega', \quad (25)$$

The source of the prompt γ is distributed over all of the BR2 core, while the sources of delayed γ are located in BR2 fuel elements or in MOX rods. After substituting expression (21) for ψ^γ into Eq.(10), the γ-heating energy can be determined as a sum

$$E_\gamma = \int_E \int_{V_B} \varphi^{p,\gamma}(r,E) H_\gamma(E) dE d^3r + \int_E \int_{V_B} \varphi_{BR2}^{d,\gamma}(r,E) H_\gamma(E) dE d^3r + \int_E \int_{V_B} \varphi_B^{d,\gamma}(r,E) H_\gamma(E) dE d^3r \quad (26)$$

here $\varphi^{p,\gamma}$, $\varphi^{d,\gamma}$ are the γ flux density determined using the Monte Carlo code MCNP from equations (23-25). Finally, the total γ-heating energy can be determined as a sum of contributors of heating energy from the prompt and delayed photons. The details of such calculations are given below.

7.2 Delayed photons from fission products in MOX rods

Equation (25) describes the transport of delayed γ from fission products in MOX rods. For the calculation of the energy deposition to the MOX rods from the delayed photons produced in β-decay reactions of fission fragments in MOX the following codes were used:

- MCNP for calculations of the fission, n_f^B, and the capture, n_c^B, reaction rates and the power in MOX rods
- SAS2H module of the SCALE-4.4a code for calculations of the source of delayed photons emitted by fission products, $q_{\gamma,B}^d(r,E)$ in Eq.(16).
- MCNP for calculation of energy deposition from this source of delayed photons, produced by fission products in the MOX rods.

The number of fission events in MOX rods, n_f^B [fiss/n], calculated using the MCNP code is normalised per one neutron emitted in fission reaction in the BR2 core. The total power in MOX rods, P_B, can be calculated using the number of fission reactions, n_f^B,

$$P_B = n_f^B Q_{eff}^B \frac{P_{BR2} \nu_{BR2}}{k_{eff} Q_{eff}^{BR2}}, \quad (27)$$

where Q_{eff}^B and Q_{eff}^{BR2} is the effective heating Q_{eff}-values for the MOX rods, and for the BR2 core respectively; ν_{BR2} is the mean number of fission neutrons produced per fission reaction in the BR2 fuel elements; P_{BR2} is the nominal power of BR2. We may expect that the ratio of Q_{eff}^B to Q_{eff}^{BR2} for the effective heating energies is close to 1.00 within the error margin of 4-5%. As a consequence of such uncertainty at the present step of calculations, the power in MOX fuel rods is determined with a similar error of 4-5%. The total intensity of delayed photons, $I_{\gamma,B}^d$ [γ/sec], emitted by fission products in MOX rods at the power P_{BR2} was calculated using the SCALE-4.4a code with the error mentioned above. We can obtain the total intensity of fissions in MOX rods, $I_{f,B}$,

$$I_{f,B} = n_f^B \frac{P_{BR2} \nu_{BR2}}{k_{eff} Q_{eff}^{BR2}}, \quad [fiss/\sec] \quad (28)$$

The number of delayed photons per fission reaction, $N_{\gamma,B}^d$, in MOX rods can be defined using the calculated intensity, $I_{\gamma,B}^d$, of delayed photons

$$N^d_{\gamma,B} = I^d_{\gamma,B}/I_{f,B} = I^d_{\gamma,B}\frac{Q^{BR2}_{eff}k_{eff}}{n^B_f P_{BR2}\nu_{BR2}}, \quad [\gamma/fiss] \qquad (29)$$

For calculation of the energy deposition, $\varepsilon^B_{\gamma,B}$ [MeV/γ] in MOX, from the delayed photons emitted by fission products in MOX fuel rods, the MCNP code was used to simulate the transport of photons from the external source of delayed photons in MOX rods. The spectrum of delayed photons was normalised per total power in MOX rods. Finally, we have the formula for calculating the contribution to the effective heating Q_{eff}-value normalized per fission reaction in MOX rods

$$Q^d_{\gamma,B} = \varepsilon^B_{\gamma,B} I^d_{\gamma,B}\frac{Q^{BR2}_{eff}k_{eff}}{n^B_f P_{BR2}\nu_{BR2}}, \quad [MeV/fiss] \qquad (30)$$

Substituting parameters calculated using the MCNP and the SAS2H module of the SCALE codes $\varepsilon^B_{\gamma,B}$=0.156 [MeV/γ], $I^d_{\gamma,B}$=3.0×10^{16} [γ/s], Q^{BR2}_{eff}=196 [MeV/fiss], n^B_f=0.00106 [fiss/n] and the nominal power P_{BR2}=60.7 [MW], ν_{BR2}=2.43 [n/fiss] we obtain the contribution from the delayed photons $Q^d_{\gamma,B}$=0.94 [MeV/fiss]. The energy of delayed photons calculated using the SAS2H module and normalized per fission reaction is two times lower than the total energy released with delayed photons in fission of ^{239}Pu (6.1 MeV/fiss). To obtain the true value of the energy released from delayed photons, we can correct the calculated intensity $I^d_{\gamma,B}$ by two times, which gives us the corrected value of $Q^{d,corr}_{\gamma,B}$=1.88 MeV/fiss. As can be seen, the contribution to the effective heating value from the delayed photons emitted by fission products in the MOX fuel rods is considerably less than the energy E^d_γ =7.2 MeV/fiss released with delayed γ in ^{235}U (see Table 7).

7.3 *Delayed photons emitted by fission products in BR2 fuel elements*

Equation (24) is used to calculate the transport of delayed photons from fission products in BR2 fuel elements and their contribution to the heating energy in MOX rods normalised per fission event in MOX fuel.

The total intensity of delayed photons emitted by BR2 fuel elements, $I^d_{\gamma,BR2}$, was calculated using the SAS2H module in the SCALE-4.4a code and re-normalised per nominal BR2 power

$$I^d_{\gamma,BR2} = \frac{P_{BR2}}{P_s} I^d_{\gamma,s}, \quad [\gamma/\mathrm{sec}] \qquad (31)$$

where P_s and $I^d_{\gamma,s}$ are the thermal power and the intensity of delayed photons generated in the BR2 fuel element. The mean heating energy, $\varepsilon^B_{\gamma,BR2}$ [MeV/γ], in the MOX fuel rods caused by delayed photons emitted from the BR2 fuel elements was calculated using the MCNP code for the external γ-source distributed in BR2 fuel elements. Using the expression for the total number of fission neutrons I^{BR2}_n generated in the BR2 core

$$I^{BR2}_n = \frac{P_{BR2}\nu_{BR2}}{Q^{BR2}_{eff}k_{eff}}, \quad [n/\mathrm{sec}] \qquad (32)$$

we obtain the number of delayed photons per fission neutron, n^{BR2}_γ,

$$n^{BR2}_\gamma = \frac{I^d_{\gamma,BR2}}{I^{BR2}_n} = \frac{I^d_{\gamma,s}Q^{BR2}_{eff}k_{eff}}{P_s\nu_{BR2}}, \quad [\gamma/n] \qquad (33)$$

To re-normalise the heating energy $\varepsilon^B_{\gamma,BR2}$ per fission in MOX rod, the number of fission reactions n_f^B in MOX rods per fission neutron in BR2 was calculated using the MCNP code. Finally, we have the following expression for the heating energy in MOX rods

$$Q^d_{\gamma,BR2} = \frac{\varepsilon^B_{\gamma,BR2} n^{BR2}_{\gamma}}{n^B_f} = \frac{\varepsilon^B_{\gamma,BR2} I^d_{\gamma,s} Q^{BR2}_{eff} k_{eff}}{P_s n^B_f \nu_{BR2}} \qquad [MeV / fiss] \qquad (34)$$

In the considered problem the following parameters were calculated: $\varepsilon^B_{\gamma,BR2}$=2.39×10^{-4} MeV/γ; $I^d_{\gamma,s}$=4.75×10^{17} γ/sec, P_s=2.0 MW; n_f^B=1.06×10^{-3} fiss/n; ν_{BR2}=2.43 n/fiss. Substituting the corresponding values to the expression for $Q^d_{\gamma,BR2}$, we obtain a contribution of delayed photons emitted by BR2 fuel elements equal to $Q^d_{\gamma,BR2}$=0.69 MeV/fiss, normalised per fission event in the MOX fuel rods. As was noted early the energy released with delayed photons which was calculated using the SAS2H module of the SCALE code is less than the total energy of delayed photons. We can correct this by increasing the intensity of delayed photons. For the model of the BR2 fuel element this correction factor is equal to 2.2. After applying this correction, the contribution of delayed photons will be equal to $Q^{d,corr}_{\gamma,BR2}$=1.52 MeV/fiss.

7.4 Average energy of fission fragments and betas in MOX rods

MOX fuel contains mixture of U and Pu nuclides. To calculate the mean kinetic energy of fission fragments and β-particles in MOX the following method was used. Using the fission rates, n_f^i, for constituent nuclides *i* and total energies E_k, E_β for U and Pu nuclides (from Table 7) we determine the average energy of fission fragments and β-particles, $Q_{k\beta}$, for the MOX fuel rods. The relative fractions of fission reactions for different fuel rods were calculated using the MCNP code and are presented in Table 8.

Table 8. Relative fractions of fission reactions for each nuclide in MOX fuel rods and the average energy $Q_{k\beta}$ for fission fragments and β-particles.

	^{235}U	^{238}U	^{239}Pu	^{241}Pu	$Q_{k\beta}$, MeV/fiss
$E_{k+\beta}$, MeV/fiss	173.2	175.8	178.9	179.6	
	Fraction of fission reactions on nuclide				
Rod A	0.023	0.026	0.774	0.167	177.0
Rod B	0.023	0.030	0.773	0.167	177.5
Rod C	0.023	0.026	0.775	0.170	177.7
Rod D	0.020	0.025	0.815	0.132	177.4
Rod E	0.020	0.031	0.811	0.127	176.8
Rod F	0.020	0.026	0.813	0.133	177.4
Rod G	0.020	0.023	0.822	0.128	177.6
Rod H	0.020	0.028	0.818	0.125	177.2
Rod I	0.020	0.023	0.823	0.127	177.6
Average for all rods					177.3

7.5 *Heating energy of prompt photons*

Equation (23) describes the transport of prompt photons from the source q_γ^p (14). The source of prompt photons is calculated in the MCNP automatically for fission and neutron capture reactions. The contribution of prompt photons to the effective heating energy per fission is considered below separately for the BR2 core and for MOX rods.

7.5.1 Heating energy of prompt γ in BR2 core.

The heating energy for prompt photons in all of the BR2 core was calculated using the MCNP code. The calculated energy includes the contribution from prompt photons emitted in fission and capture reactions in the BR2 core and is equal to 4.74 MeV/neutron. The corresponding total number of fission events in the reactor core for the BR2 model is equal to 0.423 fissions/neutron. Using these data we can evaluate the heating energy for prompt γ, Q_γ^{BR2}=11.2 MeV/fission (=4.74/0.423).

Effective fission heating energy, Q_{eff}^{BR2}, normalised per fission event in the BR2 core can be calculated easily taking into account that the fuel is mainly ^{235}U and all kinetic energy of fission fragments, the energy of β-particles and the energy of delayed photons are deposited in the core. The corresponding heating values are presented in Table 7. Using Table 7 and q_γ^{BR2} , we can obtain the total value of Q_{eff}^{BR2} =Q_F+Q_γ^{BR2}+E_n=196.4 MeV/fiss (for ^{235}U Q_F=180.4 MeV/fiss [4], E_n=4.8 MeV/fiss).

7.5.2 Test problem for an infinite mixture of ^{239}Pu and ^{238}U

To verify the accuracy of the MCNP calculation of absorbed energy from prompt photons, let us consider a very large medium of mixture of ^{239}Pu and ^{238}U (with enrichment of 9.09%). In this problem the kinetic energy of all prompt photons is deposited in the mixture. For comparison with the direct MCNP calculation, the total heating energy generated by prompt photons was calculated using the fission, n_f^i, and capture, n_c^i, reaction rates for nuclides (i=U, Pu) and the total energy of prompt photons. Table 9 contains the results of MCNP calculations for reaction rates and the energy, E_γ^{tot} , deposited by prompt photons in the test problem.

Table 9. Reaction rates and the absorbed energy of prompt photons per fission event calculated using the MCNP code for the test problem.

Nuclide	Fission rate, n_f^i, fiss/n	Capture rate, n_c^i, cap/n	Gamma heating, E_γ^{tot} MeV/n
^{238}U	0.11333	0.37967	
^{239}Pu	0.39145	0.04457	
Mixture	0.50478	0.42424	6.9

This alternative method of the calculating the heating energy is based on an assumption that all energy of prompt photons is dissipated in the medium. To perform the calculation we have to know the number of fission and capture reactions and the energy of emitted photons. We will use the effective energy released in fission and capture reactions published in the work of M.F.James [4]: $E_{\gamma,U8}^f$=7.5 MeV/fission, $E_{\gamma,Pu9}^f$=7.7 MeV/fission; $E_{\gamma,U8}^c$=5.69 MeV/capture, $E_{\gamma,Pu9}^c$=6.53 MeV/capture. The total heating energy is calculated using the formula

$$E_\gamma^{tot} = \sum_{i=U8,Pu9} \left(E_{\gamma,i}^f n_f^i + E_{\gamma,i}^c n_c^i \right), \qquad (35)$$

where $E_{\gamma,i}^f$, $E_{\gamma,i}^c$ are the energies of prompt photons emitted in fission and capture reactions, n_f^i and n_c^i are the number of fission and capture reactions per fission neutron for each nuclide i=^{238}U,^{239}Pu. From the equation (35) we obtain E_γ^{tot}=6.3 MeV/neutron, while in the MCNP calculation we have E_γ^{tot}=6.9 MeV/neutron. This comparison may be accepted as satisfactory, taking into account that different methods and different data were used in the calculations.

7.5.3 *Average heating energy of prompt photons in MOX fuel rods*

Equation (23) also is used to calculate the heating energy of prompt photons, q_γ^B, in the meat of MOX fuel rods. This is done directly using the MCNP code with initial normalisation per one fission neutron from the BR2 core (the diameter of the fuel meat is equal to 0.824 cm). The heating energy can be re-normalized per fission event in the MOX fuel, Q_γ^B, using the calculated number of fission reactions in MOX rods per fission neutron, n_f^B [fiss/n]. In Table 10 the heating energy of prompt photons, Q_γ^B, for each of the MOX rods was calculated as a ratio of q_γ^B to n_f^B.

Table 10. Heating energy of prompt photons and the number of fission reactions in MOX rods, Q_γ^B, is normalised per fission in MOX.

Fuel rod	q_γ^B, MeV/neutron	n_f^B, fission/neutron	Q_γ^B, MeV/fission
A	1.591×10^{-3} (0.45%)	$(1.312\pm0.01)\times10^{-4}$	12.12±0.11
B	1.562×10^{-3} (0.46%)	$(1.159\pm0.01)\times10^{-4}$	13.48±0.12
C	1.548×10^{-3} (0.47%)	$(1.325\pm0.01)\times10^{-4}$	11.68±0.11
D	1.368×10^{-3} (0.50%)	$(1.282\pm0.01)\times10^{-4}$	10.67±0.10
E	1.276×10^{-3} (0.50%)	$(0.980\pm0.01)\times10^{-4}$	13.03±0.12
F	1.308×10^{-3} (0.50%)	$(1.202\pm0.01)\times10^{-4}$	10.88±0.10
G	1.198×10^{-3} (0.50%)	$(1.238\pm0.01)\times10^{-4}$	9.68±0.10
H	1.099×10^{-3} (0.60%)	$(0.964\pm0.01)\times10^{-4}$	11.40±0.10
I	1.081×10^{-3} (0.60%)	$(1.144\pm0.01)\times10^{-4}$	9.45±0.10
TOTAL	1.203×10^{-2}	1.0606×10^{-3}	
Avarage for all rods, $\overline{Q_\gamma^B}$	1.337×10^{-3}	1.178×10^{-4}	11.3

The average heating energy $\overline{Q_\gamma^B}$ in the MOX fuel rods includes the contribution from prompt photons emitted in fission and neutron capture reactions, $\overline{Q_\gamma^B}$ =11.3 MeV/fiss and normalised per fission in MOX rods.

7.6 Total effective heating energy in MOX fuel rods

The total effective heating energy in MOX fuel rods normalised per fission in MOX is defined as the sum of the following components: the average energy of fission fragments and the energy of beta-particles, $Q_{k\beta}$; the heating energy from prompt photons, $\overline{Q}_{\gamma}^{B}$; the heating energy of delayed photons emitted by BR2, $Q_{\gamma,BR2}^{d}$, and by MOX fuel elements, $Q_{\gamma,B}^{d}$. The loss of the kinetic energy of fission neutrons in the rods is very small and we neglect its contribution. The effective heating energy for MOX rods was thus calculated using the formula

$$Q_{eff}^{B} = Q_{k\beta} + Q_{\gamma,B}^{d} + Q_{\gamma,BR2}^{d} + \overline{Q}_{\gamma}^{B}. \qquad (36)$$

Each component in this expression was calculated in the previous sections and was collected in Table 11.

Table 11 Contribution of various energy components to the total effective heating energy Q_{eff}^{B} for MOX fuel rods normalized per fission in MOX rods.

Component	MeV/fiss
Average energy of fission fragments and betas, $Q_{k\beta}$	177.3
Average heating energy of delayed photons emitted by fission products in MOX rods, $Q_{\gamma,B}^{d}$	0.94
Average heating energy of delayed photons emitted by fission products in BR2 fuel elements, $Q_{\gamma,BR2}^{d}$	0.69
Average heating energy of prompt photons, $\overline{Q}_{\gamma}^{B}$	11.3
Effective heating energy for MOX rods, Q_{eff}^{B}	190.2

As can be seen, the contribution from the delayed photons produced in the BR2 fuel elements to the heating in the Callisto loop is relatively small, because of the large distance between the BR2 fuel elements and MOX rods. Moreover, the delayed photons produced in MOX rods escape from the rods and lose their energy outside the MOX rods. Nevertheless, in other more central channels surrounded by BR2 fuel elements the contribution from the delayed photons can be stronger. The influence of prompt photons to the heating in MOX rods is stronger than from delayed photons because they have a larger energy due to being produced directly in the Callisto loop in the massive stainless steel pressure tubes and in borated coling water.

The calculated effective heating energy for MOX fuel rods is equal to 190.2 MeV/fiss. The average heating energy, $Q_{\gamma,B}^{d}$=0.94 MeV/fiss, induced by delayed photons generated in MOX rods, was calculated with the systematic error of about 5%, which is less than 0.05 MeV/fiss. The influence of this systematic error on the value of the effective heating energy Q_{eff}^{B} is very small. The second systematic error is associated with the calculation of the energy of delayed photons. Using corrected values for the contribution from delayed photons emitted by fission products in BR2 fuel elements and in MOX rods ($Q_{\gamma,BR2}^{d,corr}$=1.52 MeV/fiss, $Q_{\gamma,B}^{d,corr}$=1.88 MeV/fiss) we will have $Q_{eff}^{B,corr}$=191.8 MeV/fiss. The difference between uncorrected and corrected effective heating energy is small and equal to 0.8%. For this reason in all of the calculations below we will use the uncorrected effective heating energy Q_{eff}^{B}=190.2 MeV/fiss.

8. Fission and breeding reactions in MOX fuel rods

The profile of the fuel burn-up over the length of the fuel rod is influenced by the axial distribution of the thermal neutron flux. The axial power peaking factor can reach the value of 1.6. The loss of Pu in fission reactions is partially compensated by the following breeding reactions of Pu nuclides in U&Pu fuel: $^{238}U(n,\gamma)\rightarrow{}^{239}Pu$, $^{239}Pu(n,\gamma)\rightarrow{}^{240}Pu(n,\gamma)\rightarrow{}^{241}Pu$. Table 2 contains the fission and breeding rates in each MOX fuel rods per fission neutron produced in BR2. The mean breeding ratio for all fuel rods is equal to 0.58 (produced $^{239}Pu+^{241}Pu$ / burned Pu). In the computational model the uniform distribution of the fuel concentration over the length of the MOX rod was used. We suppose that the fuel burn-up in MOX rods is partially compensated by the breeding reactions.

Table 12 Reaction rates in MOX fuel rods per fission neutron.

Rod name (place)	Total fissions, fissions/neutron	Breeding of $^{239}Pu+^{241}Pu$, nucl/neutron	Ratio, Breeding / fission
F6547 (A)	1.312×10^{-4} (0.75%)	8.27×10^{-5} (1.5%)	0.63
F6548 (B)	1.159×10^{-4} (0.81%)	7.37×10^{-5} (1.7%)	0.64
F6549 (C)	1.325×10^{-4} (0.86%)	8.06×10^{-5} (1.5%)	0.61
F6680 (D)	9.800×10^{-5} (0.98%)	6.84×10^{-5} (1.7%)	0.70
F6678 (E)	1.202×10^{-4} (0.90%)	5.81×10^{-5} (2.0%)	0.48
F6677 (F)	1.238×10^{-4} (0.90%)	6.48×10^{-5} (1.8%)	0.52
F6673 (G)	9.641×10^{-5} (1.00%)	6.52×10^{-5} (1.7%)	0.68
F6679 (H)	1.312×10^{-4} (0.75%)	5.48×10^{-5} (1.7%)	0.42
F6674 (I)	1.312×10^{-4} (0.75%)	6.16×10^{-5} (1.7%)	0.47
Sum	1.0606×10^{-3}	6.100×10^{-4}	0.58

9. Validation of the BR2 model

9.1 Heating energy in CALLISTO loop

The results of measuring the gamma heating in the CALLISTO loop were published in [8]. The measurement was performed for the stainless steel rods equivalent to the MOX rods in the cycle 02/97B. The thermal balance method was used to determine the gamma heating inside the CALLISTO loop. Comparison of the measured and calculated heating energy is shown in Table 13. The power determined by the thermal balance method is equal to 27.8 kW. The calculated power, P_γ^B =26.5 kW, includes the heating by prompt photons generated by all structural elements in the reactor and the contribution of the delayed photons from fission products in BR2 fuel elements.

The ratio of the gamma heating energy to the total heating energy in the MOX fuel is equal to 5.9%. Taking into account the heating in the rod cladding, in water and in the spacer, this ratio becomes equal to 9.8%. The corresponding ratio in the BR2 core is equal to 5.8%. This difference may be explained by the presence of a larger amount of stainless steel 316 and boron in cooling water in the channel than in the core where the main structural materials are Al, water and Be.

Table 13 Heating energy of prompt gamma's in structural elements of the CALLISTO loop normalised per fission neutron and per fission event in MOX fuel.

	MCNP calculation			Thermal balance method [8]
Structural element	Heating energy from prompt γ per fission event. MeV/fission	Heating energy from delayed γ per fission event. MeV/fission	Power: prompt+ delayed γ kW	Power, kW
Fuel	11.3	0.9	9.7±0.2	
Fuel rods+spacer	14.8	1.06	12.6±0.2	
All device (+water)	17.7	1.10	15.0±0.2	
All device + internal pressure tube	30.8	2.3	26.5±0.5	27.8

9.2 Comparison of the thermal balance method and MCNP calculation

The power in all MOX fuel rods is determined by measuring the temperature at the inlet and outlet of the cooling water and using a thermal hydraulic analysis [6].
It should be noted that in the thermal balance method the mean linear power and the peak linear power in each fuel rod are determined using a preliminary calculated distribution of power between the various fuel rods. The radial and the axial peaking factors for fuel rods are calculated ordinary by using approximate 2-D neutron diffusion and transport computer models. For this reason the power distribution in fuel rods obtained in the thermal balance method is not

measured directly in the experiment. But the total thermal power for all fuel rods is determined directly from the experiment.

The linear power in the MOX rods is calculated using the expression (8)

$$l^{calc} = \frac{P_B}{L}, \qquad [W/cm] \qquad (37)$$

where L is the length of the fuel rod. The comparison of the calculated linear power in MOX rods, l^{calc}, and the measured one obtained from the thermal balance method , l^{th}, [6] are presented in Table 14. The mean ratio of the calculated results to the measured is equal to 0.98. This ratio indicates to the systematic error of 2% for the total power in the MOX rods calculated using the MCNP model of BR2. The relative distribution of power in various rods obtained by the thermal balance method and calculated by the MCNP model of BR2 is also in very good agreement.

Table 14 Mean linear power in MOX fuel rods measured by the thermal balance method, l^{th}, and calculated, l^{calc}, using the MCNP model. (The values in the brackets are the estimated relative standard deviation at the 1σ level)

	MCNP calculation		Thermal balance method [6]	Ratio $\frac{l^{calc}}{l^{th}}$
	n_f^B, fiss/n	l^{calc}, W/cm	l^{th}, W/cm	
F6547 (A)	1.312×10^{-4} (0.75%)	187.4	190.6	0.98
F6548 (B)	1.159×10^{-4} (0.81%)	165.5	169.9	0.97
F6549 (C)	1.325×10^{-4} (0.86%)	189.3	192.8	0.98
F6680 (D)	9.800×10^{-5} (0.98%)	183.1	181.2	1.01
F6678 (E)	1.202×10^{-4} (0.90%)	140.0	142.6	0.98
F6677 (F)	1.238×10^{-4} (0.90%)	171.7	180.4	0.95
F6673 (G)	9.641×10^{-5} (1.00%)	176.8	176.2	1.00
F6679 (H)	1.312×10^{-4} (0.75%)	137.7	141.6	0.97
F6674 (I)	1.312×10^{-4} (0.75%)	163.4	173.8	0.94
Mean value for all rods		168.3	172.1	0.98

The comparison of the peak linear power in fuel rods is presented in Table 15. The mean ratio of the calculated peak linear power, m^{calc}, and obtained from the thermal balance method, m^{th}, is equal to 1.04. This means that the power peaking factors used in the thermal balance method are close to the factors calculated using the MCNP model of BR2.

Table 15 Comparison of the calculated, m^{calc}, peak linear power in MOX fuel rods and obtained in the thermal balance method, m^{th}.

	MCNP calculation	Thermal balance method [6]	Ratio
Name of rod	m^{calc}, W/cm	m^{th}, W/cm	m^{calc}/m^{th}
F6547 (A)	312±12	295	1.06±0.04
F6548 (B)	274±11	263	1.04±0.04
F6549 (C)	326±11	297	1.10±0.04
F6680 (D)	304±11	293	1.04±0.04
F6678 (E)	244±11	232	1.05±0.04
F6677 (F)	286±13	291	0.98±0.04
F6673 (G)	294±13	286	1.03±0.04
F6679 (H)	245±12	230	1.07±0.04
F6674 (I)	282±13	282	1.00±0.04
Mean			1.04

9.3 Comparison of the gamma-spectrometric measurements and calculated distribution of fission rate in MOX rods

9.3.1 Total fission rate

The total fission rate in MOX rods was measured after the irradiation cycle 05/98a using the γ-spectrometer and published in the SCK-CEN report [1]. The total fission rates, $I_{f,B}^{calc}$, in MOX rods were calculated using the MCNP model

$$I_{f,B}^{calc} = n_f^B \frac{P_{BR2} V_{BR2}}{Q_{eff}^{BR2} k_{eff}}, \qquad n_f^B = \sum_i \int_E \int_{V_B} n_i \sigma_f^i(E) \Phi(E) dE dr, \tag{38}$$

here n_f^B is the fission rate in the rods per fission neutron.
Comparison of the total fission rates measured by the γ-spectrometric method and calculated using the MCNP model of BR2 is shown in Table 16. The calculated fission rate is normalised per nominal power of BR2 in cycle 05/98a.

The mean ratio of the calculated fission rate to the measured value obtained by the γ-spectrometric method is equal to 0.94. The systematic deviation of 6% is comparable with the experimental error that is equal to 4.4% [1].

Table16 Comparison of the total fission rate in MOX fuel rods measured by the γ-spectrometric method, $I_{f,B}^{exp}$, and calculated by using the MCNP code, $I_{f,B}^{calc}$. The mean fission rate $\bar{I}_{f,B}^{exp}$ is equal to the mean value of the high and the low measured values of the fission rate (the numbers in the brackets are the relative errors.)

	n_f^B (MCNP), (error)	$I_{f,B}^{calc}$	$I_{f,B}^{exp}$ High , Low, (error)	$\bar{I}_{f,B}^{exp}$	$I_{f,B}^{calc} / \bar{I}_{f,B}^{exp}$
Name of rod	fiss/n	fiss/sec	Fiss/sec	Fiss/sec	Ratio*)
F6547 (A)	1.312×10^{-4} (0.75%)	6.15×10^{14}	7.14×10^{14} 6.54×10^{14} (4.3%)	6.84×10^{14}	0.90 ± 0.05
F6548 (B)	1.159×10^{-4} (0.81%)	5.45×10^{14}	6.07×10^{14} 5.56×10^{14} (4.4%)	5.81×10^{14}	0.94 ± 0.05
F6549 (C)	1.325×10^{-4} (0.86%)	6.21×10^{14}	6.87×10^{14} 6.31×10^{14} (4.3%)	6.59×10^{14}	0.94 ± 0.05
F6680 (D)	9.800×10^{-5} (0.98%)	6.01×10^{14}	6.63×10^{14} 6.08×10^{14} (4.4%)	6.36×10^{14}	0.94 ± 0.05
F6678 (E)	1.202×10^{-4} (0.90%)	4.59×10^{14}	4.96×10^{14} 4.54×10^{14} (4.4%)	4.75×10^{14}	0.97 ± 0.05
F6677 (F)	1.238×10^{-4} (0.90%)	5.64×10^{14}	6.42×10^{14} 5.89×10^{14} (4.3%)	6.16×10^{14}	0.92 ± 0.05
F6673 (G)	9.641×10^{-5} (1.00%)	5.80×10^{14}	6.45×10^{14} 5.91×10^{14} (4.3%)	6.18×10^{14}	0.94 ± 0.05
F6679 (H)	1.312×10^{-4} (0.75%)	4.52×10^{14}	4.95×10^{14} 4.53×10^{14} (4.4%)	4.74×10^{14}	0.95 ± 0.05
F6674 (I)	1.312×10^{-4} (0.75%)	5.36×10^{14}	6.09×10^{14} 5.58×10^{14} (4.3%)	5.83×10^{14}	0.92 ± 0.05
Mean					0.94 ± 0.05

*) The error of a quotient r=A/B was calculated using

$\frac{\delta r}{r} = \frac{\delta A}{A} + \frac{\delta B}{B}$, where δA/A is the relative error of value A.

9.3.2 Peak fission rate

The measured peak fission rate, $M_{f,B}^{exp}$, is obtained using the measured total fission rate, $I_{f,B}^{exp}$, and the shape factors, k_z^{exp}, determined in γ-spectrometric measurements [1]

$$M_{f,B}^{exp} = k_z^{exp} I_{f,B}^{exp} / L, \quad \left[\frac{fiss}{\sec.mm}\right] \qquad (39)$$

The shape factors for the fission rate distribution are presented in Table 17. In Table 18 we compare the experimental and the theoretical (based on the MCNP model) peak fission rates. γ-Spectra were measured each millimetre over the whole length of the fuel rods. The low, high and the mean peak values of the fission rate in the maximum region are included in Table 18. The axial distribution of fissions in fuel rods were calculated using the MCNP code for axial mesh containing geometrical segments of 2 cm length. The ratio of the calculated to the measured peak fission rate for various MOX rods changes from 0.93 to 1.05. The mean value for the ratio of the theoretical and the experimental peak rates is equal to 0.99.

Table 17. Shape factors k_z^{exp} for fuel rods measured in γ-spectrometry method [1].

rod	k_z^{exp}	Rod	k_z^{exp}
F6547 (A)	1.60	F6677 (F)	1.61
F6548 (B)	1.60	F6673 (G)	1.61
F6549 (C)	1.57	F6679 (H)	1.61
F6680 (D)	1.61	F6674 (I)	1.61
F6678 (E)	1.62		

Table 18 Comparison of the peak fission rate, $M_{f,B}^{exp}$, measured by gamma-spectrometric method and calculated using the MCNP model of BR2 . The low, high and mean values of measured peak fission rate, $M_{f,B}^{exp}$, in the maximum of fission rate distribution are included in the table. $M_{f,B}^{calc}$ is the peak fission rate calculated using the MCNP model (relative statistical errors are shown in brackets).

	Gamma-spectrometry, $M_{f,B}^{exp}$			MCNP	Ratio
Rod	Peak low, Fiss/sec/mm	Peak high, fiss/sec/mm	Peak mean, fiss/sec/mm	Peak, $M_{f,B}^{calc}$ fiss/sec/mm	$\frac{M_{f,B}^{calc}}{M_{f,B}^{exp}}$
F6547 (A)	10.49×10^{11}	11.46×10^{11}	11.0×10^{11}	10.24×10^{11} (4.4%)	0.93
F6548 (B)	8.91×10^{11}	9.73×10^{11}	9.32×10^{11}	9.00×10^{11} (4.9%)	0.97
F6549 (C)	9.95×10^{11}	10.8×10^{11}	10.4×10^{11}	10.7×10^{11} (4.4%)	1.03
F6680 (D)	9.80×10^{11}	10.69×10^{11}	10.2×10^{11}	9.97×10^{11} (4.9%)	0.97
F6678 (E)	7.36×10^{11}	8.04×10^{11}	7.70×10^{11}	8.00×10^{11} (5.6%)	1.04
F6677 (F)	9.49×10^{11}	10.34×10^{11}	9.92×10^{11}	9.39×10^{11} (5.0%)	0.95
F6673 (G)	9.57×10^{11}	10.44×10^{11}	10.0×10^{11}	9.65×10^{11} (5.0%)	0.97
F6679 (H)	7.30×10^{11}	7.98×10^{11}	7.64×10^{11}	8.04×10^{11} (6.0%)	1.05
F6674 (I)	9.05×10^{11}	9.87×10^{11}	9.46×10^{11}	9.25×10^{11} (5.2%)	0.98
Mean					0.99

9.4 Comparison of the γ-spectrometric and the thermal balance methods

The mean linear power, l^{γ}, in the fuel rod was determined using the measured fission rates, $I^{exp}_{f,B}$, in the γ-spectrometric method and the effective heating energy Q^{B}_{eff}=190.2 [MeV/fiss] for MOX fuel rods

$$l^{\gamma} = I^{exp}_{f,B} Q^{B}_{eff} / L, \qquad [W/cm] \qquad (40)$$

here L is the length of fuel in the rod. Comparison with the thermal balance method is presented in Table 19. The difference in the linear power obtained by two methods belongs to the spread range 1.01 – 1.09. The mean deviation of the γ-spectrometry results from the thermal balance method (TBM) is equal to 1.047.

Table 19. Comparison of the mean linear power measured by the γ-spectrometric and the thermal balance methods. The mean linear power $\bar{l}^{\gamma}$ is equal to $(l^{\gamma}_{high} + l^{\gamma}_{low})/2$.

	Gamma-spectrometry			Thermal balance method (TBM)	Ratio $\bar{l}^{\gamma} / l^{th}$
Rod	Fission rate high, low [1]	Linear power high, low	Mean linear power	Mean linear power [6]	Spectrometry/ TBM
	$I^{exp}_{f,B}$ *(high)* *(low)*	l^{γ}_{high} l^{γ}_{low}	$\bar{l}^{\gamma}$	l^{th}	
	Fiss/sec	W/cm	W/cm	W/cm	Ratio
F6547 (A)	7.14×10^{14} 6.54×10^{14}	217.6 199.3	208.4	190.6	1.093
F6548 (B)	6.07×10^{14} 5.56×10^{14}	185.0 169.4	177.2	169.9	1.043
F6549 (C)	6.87×10^{14} 6.31×10^{14}	209.3 192.3	200.8	192.8	1.041
F6680 (D)	6.63×10^{14} 6.08×10^{14}	202.0 185.3	193.6	181.2	1.068
F6678 (E)	4.96×10^{14} 4.54×10^{14}	151.1 138.3	144.7	142.6	1.015
F6677 (F)	6.42×10^{14} 5.89×10^{14}	195.6 179.5	187.5	180.4	1.039
F6673 (G)	6.45×10^{14} 5.91×10^{14}	196.5 180.0	188.3	176.2	1.069
F6679 (H)	4.95×10^{14} 4.53×10^{14}	150.8 138.0	144.4	141.6	1.020
F6674 (I)	6.09×10^{14} 5.58×10^{14}	185.6 170.0	177.8	173.8	1.023
Mean			180.3	172.1	1.047

The peak linear power, m^{th}, in fuel rods in the γ-spectrometry method was determined using the peak fission rate, $M_{f,B}^{exp}$, and the effective heating value, Q_{eff}^{B}=190.2 MeV/fiss, calculated for the MOX fuel rods

$$m^{th} = M_{f,B}^{exp} Q_{eff}^{B}, \qquad [W/cm] \tag{41}$$

The comparison of the peak linear power obtained by both methods is presented in Table 20. The ratio of the peak linear power in fuel rods obtained by the γ-spectrometry method to the values in the thermal balance method is denoted by $\overline{m^{\gamma}}/m^{th}$. This ratio for various rods varies from 0.97 to 1.13. The mean ratio for all rods is equal to 1.05.

As was indicated earlier, the mean ratio defines the difference in the total power in all fuel rods. The systematic deviation of 5% observed in the present calculations between the gamma-spectrometry and the thermal balance methods is comparable with the experimental error in the γ-spectrometric method. The error of determining the linear power in the thermal balance method is about 7-8%.

Table 20. Comparison of the peak linear power measured by the gamma-spectrometry and the thermal balance methods.

	Gamma-spectrometry			Thermal balance method (TBM)	Ratio
Rod	peak fission rate high-low [1]	peak linear power high-low [1]	Peak linear power, mean	Peak linear power [6]	Spectrometry / TBM
	$M_{f,B}^{exp}$ *(high)* *(low)*	m_{high}^{γ} m_{low}^{γ}	$\overline{m^{\gamma}}$	m^{th}	$\overline{m^{\gamma}}/m^{th}$
	Fiss/sec/mm	W/cm	W/cm	W/cm	Ratio
F6547 (A)	11.40×10^{11} 10.49×10^{11}	347.4 319.6	333.5	295	1.13
F6548 (B)	9.73×10^{11} 8.92×10^{11}	296.5 271.8	284.2	263	1.08
F6549 (C)	10.80×10^{11} 9.95×10^{11}	329.0 303.2	316.1	297	1.06
F6680 (D)	10.68×10^{11} 9.80×10^{11}	325.4 298.6	312.0	293	1.06
F6678 (E)	7.98×10^{11} 7.30×10^{11}	243.2 222.4	232.8	232	1.00
F6677 (F)	10.33×10^{11} 9.48×10^{11}	314.8 288.9	301.9	291	1.04
F6673 (G)	10.44×10^{11} 9.57×10^{11}	318.1 291.6	304.9	286	1.07
F6679 (H)	7.98×10^{11} 7.30×10^{11}	243.2 222.4	232.8	230	1.01
F6674 (I)	9.82×10^{11} 8.24×10^{11}	299.2 251.7	275.5	282	0.97
Mean					1.05

10. Conclusion

Benchmark calculations of the fission rate distribution in the MOX fuel rods irradiated in cycle 05/98a were performed using the realistic model of BR2 by using the MCNP code. The effective heating energy for MOX fuel rods was calculated using the MCNP and SCALE codes, taking into account the contributions from the prompt and delayed photons. The linear power in the MOX fuel rods is determined by using the fission rate distribution and the effective heating energy in MOX fuel rods.

Three methods of defining the irradiation conditions of MOX fuel rods are compared:
- the thermal balance measurements;
- gamma-spectrometric measurements;
- theoretical calculations of the fission rate, of the effective heating energy and the linear power in rods.

Results of comparison of all these methods are presented below.

10.1 Fission rate in MOX rods

Comparison of γ-spectrometric measurements and MCNP calculations

The distribution of the fission rate in MOX fuel rods was calculated using the MCNP model of BR2 and measured by the γ-spectrometry method. The Table below contains the ratio of the calculated fission rates to the corresponding values measured by the γ-spectrometry method.

Compared parameter	Ratio of MCNP calculations to γ-spectrometry method	
	Range for all rods	Average for 9 rods
Total fission rate in rods	0.90 ÷ 0.97	0.94 ± 0.05
Peak fission rate in rods	0.93 ÷ 1.05	0.99 ± 0.05

The total fission rate in MOX rods calculated using the MCNP model of BR2 is systematically lower by 6% than the rate measured by the γ-spectrometry method. The maximum of the fission rate in the BR2 calculation model coincides with the γ-spectrometry results within the error margin of ± 5%. The error of the γ-spectrometry results is equal to 4.4% [1].

10.2 Linear thermal power in MOX rods

a) Comparison of the thermal balance measurements and MCNP calculations

Compared parameter	Ratio of MCNP calculations to thermal balance method	
	Range for all rods	Average for 9 rods
Mean linear thermal power	0.94 ÷ 1.01	0.98
Peak linear thermal power	0.98 ÷ 1.10	1.04

The mean linear power calculated using the MCNP model of BR2 is systematically lower by 2% than the power measured in the thermal balance method.

The peak linear power in calculations is higher than expected from the thermal balance method by 4%. This means that the peaking factors used in the thermal balance method are similar to the calculated factors using the MCNP code.

b) Comparison of the γ-spectrometry and the thermal balance methods

Compared parameter	Ratio of γ-spectrometry to thermal balance results	
	Range	Average for 9 rods
Mean linear thermal power	1.01 ÷ 1.09	1.05
peak linear thermal power	0.97 ÷ 1.13	1.05

The mean linear power determined using the fission rate measured in the γ-spectrometry analysis and using the calculated effective heating energy for MOX rods (190.2 MeV/fiss) differs from the thermal balance method by 5%.

As can be seen from the presented analysis, the γ-spectrometry measurements, the thermal balance measurements and the theoretical model of BR2 reactor give the average deviation between them of about 5-6% for the fission rate distribution, for the linear power and for the peak linear power in fuel rods.

Acknowledgement

The authors would like to thank P.Gubel, M.Verwerft for their encouragement in this work, and M.Weber, L.Vermeeren, A .Beeckmans for useful discussions.

References

[1] L.Borms, BACCHANAL PIE Campain 3. Gamma Spectroscopy. SCK-CEN, R-3496, February 2001.
[2] Ch.De Raedt, E.Malambu, CALLISTO 1997 (cycle01/97a): Neutronic calculations performed by SCK-CEN.Situation April 30, 1997. SCK-CEN Report TN-0005, June 1997.
[3] E.Malambu, Ch.De Raedt, M.Weber, Assessment of the linear power level in fuel rods irradiated in the CALLISTO loop in the high flux materials testing reactor BR2, Report SCK-CEN, P-12, 1999.
[4] M.F.James, Energy released in fission., J.Nucl.Energy, 1969, v23, n.9, p 517.
[5] MCNP^{TM} – A General Monte Carlo N-Particle Transport Code. Vertion 4c. J.F.Breismeister. LA-13709-M
[6] P.Benoit, M.Weber, Boucle CALLISTO, Rapport du cycle 05/98, Irradiation du 4.12.98 ua 23.12.98, SCK-CEN Technical Note MI.57/D088010/12/PB/MW.rw, 15 Feb.1999.
[7] T.Graham, M.Weber, The CALLISTO project, SCK-CEN Technical Note NT.56/B1400/79/TG/MW, 28 April 1993.
[8] M.Weber, CALLISTO: Mesure de l'echauffement gamma dans les IPS, SCK-CEN Memo Interne, MI.57/D088010/74/MW.rw, Revision A, 8 February 1999.

List of Symbols

E_k – is the average kinetic energy of fission fragments [MeV/fiss];

E_γ^f - initial kinetic energy of prompt photons produced in fission reaction [MeV/fiss];

E_γ^d - average kinetic energy of delayed photons produced in decay of fission products [MeV/fiss];

E_β- mean total kinetic energy of β-particles emitted by fission products [Mev/fiss];

E_n – average energy of fission neutrons [MeV/fiss];

$E_{\gamma,i}^f$ – energy of prompt photons emitted in fission of nuclide i [MeV/fiss];

$E_{\gamma,i}^c$ – energy of prompt photons emitted in reaction of neutron capture in nuclide i and normalized per capture reaction [MeV/capt];

E_γ^{tot} – total energy of prompt photons [MeV/n] in the test problem;

E_γ is the heating energy of photons [MeV];

E_{BR2} - energy produced in the BR2 [J];

$\varepsilon_{\gamma,B}^B$ – is the mean heating energy in MOX fuel rods caused by delayed photons produced in MOX rods [MeV/γ]; normalized per delayed photon emitted by fission products in MOX rods;

$\varepsilon_{\gamma,BR2}^B$ – is the mean heating energy in MOX fuel rods caused by delayed photons produced by BR2 fuel elements; normalized per delayed photon emitted from BR2 fuel element [MeV/γ];

$H_\gamma(E)$ is the γ-heat response;

I_n^{BR2} – total intensity of fission neutrons generated in BR2 core [n/sec];

$I_{f,B}$ – total intensity of fission reactions in MOX fuel rods normalized per total power P_B in MOX rods [fiss/sec];

$I_{\gamma,B}^d$ – intensity of delayed photons emitted by fission fragments in MOX fuel rods; Normalized per total power P_B in MOX rods [γ/sec];

$I_{\gamma,s}^d$ – is the intensity of delayed photons emitted by single BR2 fuel element. Normalized per thermal power P_S in BR2 fuel element [γ/sec];

$I_{\gamma,BR2}^d$ - is the total intensity of delayed photons emitted by BR2 fuel elements normalized per nominal power of BR2 [γ/sec];

$K_\gamma(r', E', \Omega' \to r, E, \Omega)$ is the kernel describing the interaction of γ with material;

k_z - is the shape factor for the axial distribution of fission rate in MOX rods measured by the γ-spectrometry method [fiss/sec];

l^γ - is the mean linear power in MOX rods measured by the γ-spectrometry method;

l^{calc} - calculated linear power in MOX rods;

l^{th} - linear power in MOX rods measured in the thermasl balance method [W/cm];

$\bar{l}^\gamma$ - mean linear power in MOX rods measured by γ-spectrometry method [W/cm];

L - is the length of MOX rod;

m^{calc} - the calculated peak linear power in MOX rods [W/cm];

m^γ - the peak linear power in MOX rods measured by the γ-spectrometry method [W/cm];

m^{th} - the peak linear power obtained in the thermal balance method [W/cm];

$\overline{m}^{\gamma}$ - the peak linear power measured by the γ-spectrometry method [W/cm];

$M_{f,B}^{calc}$ - peak fission rate calculated using the MCNP model [fiss/sec/mm];

$M_{f,B}^{exp}$ - peak fission rate measured by the γ-spectrometry method [fiss/sec/mm];

$N_{\gamma,B}^{d}$ – the number of delayed photons per fission reaction occurred in MOX fuel rods [γ/fiss];

n_f^B – is the number of fission events in MOX rods per fission neutron produced in BR2 [fiss/n]

n_c^B – is the number of neutron capture events in MOX rods per fission neutron produced in BR2 [cap/n]

n_{γ}^{BR2} – number of delayed photons emitted by fission fragments in BR2 fuel elements per fission neutron [γ/n];

n_f^i - is the number of fission reactions per neutron for nuclide *i*;

n_c^i - is the number of neutron capture reactions per neutron for nuclide *i*;

P_{BR2} – nominal power of BR2 [MW];

P_B – total power in MOX fuel rods normalized per nominal power of BR2 [MW];

$P_{\gamma,B}$ - power in the CALLISTO loop induced by photons;

P_S – thermal power of typical single BR2 fuel element [MW];

p_c – probability of neutron capture reaction ;

Q_{eff} – effective energy for fission reaction [MeV/fiss];

$Q_F = E_k + E_\beta + E^d_\gamma$ - fission heating Q-value {MeV/fiss] used in MCNP code;

Q_{eff}^{BR2} – effective heating energy released per fission reaction in BR2 fuel elements [MeV/fiss];

Q_{eff}^{B} – effective heating energy for MOX fuel rods normalized per fission rection in MOX rod, [MeV/fiss];

$Q_{k\beta}$ – average energy of fission fragments and β-particles for the mixture of nuclides in MOX fuel rods. Includes the kinetic energy of fission fragments and total energy of β-particles. [MeV/fiss];

Q_{γ}^{BR2} – contribution of prompt photons to the heating energy in BR2 core [MeV/fiss];

Q_{γ}^{B} – heating energy of prompt photons in MOX fuel rods normalized per fission event in MOX rod [MeV/fiss MOX];

$Q_{\gamma,BR2}^{d}$ – contribution of delayed photons produced in BR2 fuel elements to the effective heating energy in MOX fuel rods, normalized per fission in MOX [MeV/fiss];

$Q_{\gamma,B}^{d}$ – contribution of delayed photons emitted from MOX fission products to the effective heating energy in MOX rods [MeV/fiss];

q_{γ}^{B} - heating energy of prompt γ in MOX rods normalyzed per fission neutron in BR2 core [MeV/n].

q_{γ} is the source of γ: $q_{\gamma}^{p,f}$ and $q_{\gamma}^{p,c}$ for source of prompt γ in fission and capture reactions, $q_{\gamma,BR2}^{d}$ for source of delayed γ in BR2 fuel , and $q_{\gamma,B}^{d}$ - for MOX rods.

q_1^p is the density of first collisions for γ: $q_1^{p,\gamma}$ for source of prompt γ, $q_{1,BR2}^{d,\gamma}$ for source of delayed γ in BR2 fuel , and $q_{1,B}^{d,\gamma}$ - for MOX rods

$\chi_f^{p,\gamma}$ - is the spectrum of prompt γ in fission reaction;

$\chi_c^{p,\gamma}$ - is the spectrum of prompt γ in neutron capture reaction;
$\chi_f^{d,\gamma}$ - is the spectrum of delayed γ in fission reaction;

S_n – number of fission neutrons in BR2 normalysed per nominal power P_{BR2} [n];
$T_\gamma(r' \rightarrow r; E, \Omega)$ is the kernel describing the γ transport;
$\varphi^\gamma(r,E)$ is the γ-flux density: $\varphi^{p,\gamma}$ for source of prompt γ, $\varphi_{BR2}^{d,\gamma}$ for source of delayed γ in BR2 fuel , and $\varphi_B^{d,\gamma}$ - for MOX rods;
$\psi^\gamma(r,E)$ is the density collision function for γ : $\psi^{p,\gamma}$ for source of prompt γ, $\psi_{BR2}^{d,\gamma}$ for source of delayed γ in BR2 fuel, and $\psi_B^{d,\gamma}$ - for MOX rods;

ν_{BR2} – mean number of fission neutrons per fission event in BR2 [n/fiss];